Available online at www.sciencedirect.com
ScienceDirect
Advances in Space Research 39 (2007) 701–710
ADVANCES IN SPACE RESEARCH (a COSPAR publication)
www.elsevier.com/locate/asr

Improvement of IRI B0, B1 and D1 at mid-latitude using MARP

E. Blanch [a], D. Arrazola [a], D. Altadill [a,*], D. Buresova [b], M. Mosert [c]

[a] Observatorio del Ebro, Universidad Ramon Llull, CSIC, Carretera de l'Observatori 8, E43520 Roquetes, Spain
[b] Institute of Atmospheric Physics AS CR, Boční II 1401, 141 31 Prague 4, Czech Republic
[c] CASLEO, Casilla de Correo 467, Av. España 1512 sur, CP J5402DSP, San Juan, Argentina

Received 1 December 2005; received in revised form 10 May 2006; accepted 30 August 2006

Abstract

Comparative analysis of predicted parameters B0, B1 and D1 by IRI-2001model (International Reference Ionosphere) and those obtained from the Monthly Averaged Representative Profiles (MARP) at mid-latitude station shows significant disagreement. The linear coefficient of determination between the model-predicted and expected (MARP) values are about $R^2 \sim 0.45$, 0.22, and 0.15 for B0, B1 and D1, respectively. A Local Model (LM) created using a general least-square fit to a harmonic function of these parameters obtained by MARP simulating the diurnal, semidiurnal and seasonal variations improves the linear coefficient of determination between the expected and IRI-predicted parameters by factor of two. The coefficients obtained from this model could be implemented into the IRI software to improve calculations of the parameters B0, B1 and D1.

Keywords: Midlatitude ionosphere; Botomside electron density profiles; IRI B parameters modeling; Sunspot activity dependence

1. Introduction

The International Reference Ionosphere (IRI) was developed in the late sixties by the Committee on Space Research (COSPAR) and the International Union of Radio Science (URSI) to produce an empirical standard model of the ionosphere. For given location, time and date, IRI provides monthly averages of the ionospheric plasma parameters such as critical frequencies, heights, electron density profiles and many others. Since its creation, IRI is being improved and updated continuously with the results of the annual workshops and the special IRI Task Force Activities (TFAs). The latest version of IRI model is the IRI-2001, which undergoes numerous improvements and contains several new components (Bilitza, 2001, 2003). The most important changes are the inclusion of the Storm-Time Empirical Ionospheric Correction Model (STORM) (Araujo-Pradere et al., 2002a,b; Bilitza, 2001, 2003), as well as the inclusion of an ion drift model (Bilitza, 2001, 2003), a new F1 layer description which depends on a single parameter D1 (Reinisch and Huang, 2000), and a new table of values for the two parameters B0 and B1 which determine the bottomside thickness and shape respectively (Bilitza et al., 2000; Bilitza, 2001, 2003).

The predictions of the IRI model are tested with measured ionospheric data. The IRI predictions of the critical frequencies and heights show that IRI has a good agreement with the measured values for geomagnetically quiet periods (Soicher et al., 1995; Mosert et al., 2004). However, IRI predictions of the parameters B0, B1 and D1 are significantly in disagreement with the observed ones (Sethi and Mahajan, 2002; Lei et al., 2004), despite a number of efforts to improve the model by a series of IRI TFAs (Radicella et al., 1998).

The aim of this paper is to introduce a technique which allows better prediction of the parameters B0, B1 and D1 for single locality (local model) than the actual IRI tabular form. The Local Model (LM) is an empirical model based on a general least-square fitting of measurements to a harmonic function (Press et al., 1986). LM simulates the

* Corresponding author.
E-mail address: daltadill@obsebre.es (D. Altadill).

0273-1177/$30
doi:10.1016/j.asr.2006.08.007

diurnal, semidiurnal and seasonal variations according to different solar activity levels. The parameters B0, B1 and D1 obtained from the Monthly Averaged Representative Profile (MARP) technique (Huang and Reinisch, 1996b) have been used as inputs to create the LM. The MARPs have been computed from the retrospective database of the Ebro Observatory (40.8°N, 0.5°E) of electron density profiles N(h), that covers more than one solar cycle (1988–2004). With the above formulation, the daily, yearly and solar cycle variations are well represented for three parameters, and the linear coefficient of determination between expected (measured) and modeled parameters by LM is improved by factor of two in comparison with IRI-2001 prediction.

2. Data

We use the full database of vertical incidence ionograms from the Ebro Observatory (40.8°N, 0.5°E) recorded by a DGS 256, that covers the time interval from June 1988 to September 2005, except the large gaps of 1989 and from May to December of 1996. The ionogram's traces have been carefully revised by operator in order to avoid any mistake of the Automatic Real Time Ionogram Scaler with True Height (ARTIST) (Huang and Reinisch, 1996a) with the Digisonde Ionogram Data Visualization/Editing Tool (SAO-X). The data not scaled by operator (from 1992 to 1994) have been not considered in this study. All together we analyzed more than 12 years of N(h) profiles. Once the ionogram's traces are revised, we computed the 'true' height electron density profiles N(h) with the True Height Profile Inversion Tool (NHPC 4.30) included on SAO-X. All this software is available at the website of the Center for Atmospheric Research of the University of Massachusetts Lowell (http://ulcar.uml.edu/), and a brief description is available at Reinisch et al. (2005) and references therein. The individual profiles corresponding to a given month and a given hour have been used to obtain the corresponding MARP by the CARP software (Huang and Reinisch, 1996b), that it is available also at http://ulcar.uml.edu/. The MARPs were computed excluding the individual profiles having deviations larger than 25% in order to avoid extreme pro-

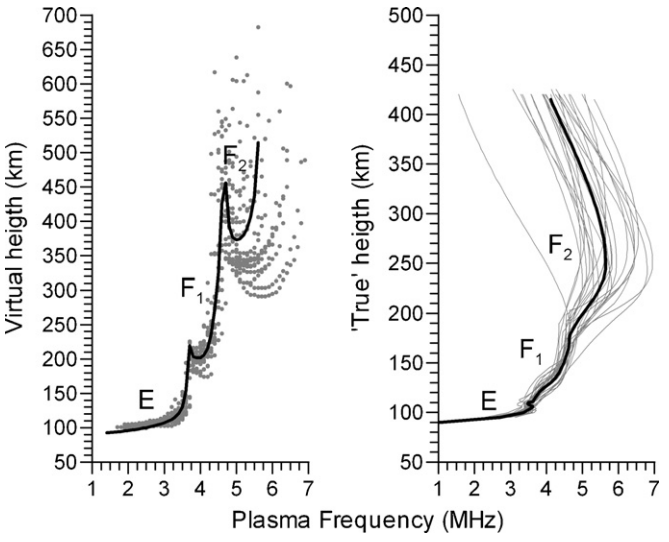

Fig. 1. An example of the MARP obtained for June 2005 at 1200 UT over Ebro station. The plot at the left shows the individual traces extracted from all days ionograms' of June 2005 recorded at 1200 UT (grey dots), and the computed trace of the MARP (thick black line). The plot at the right depicts the 'true height' plasma frequency profiles computed for all days of June 2005 at 1200 UT (grey thin lines), and the corresponding MARP (thick black line).

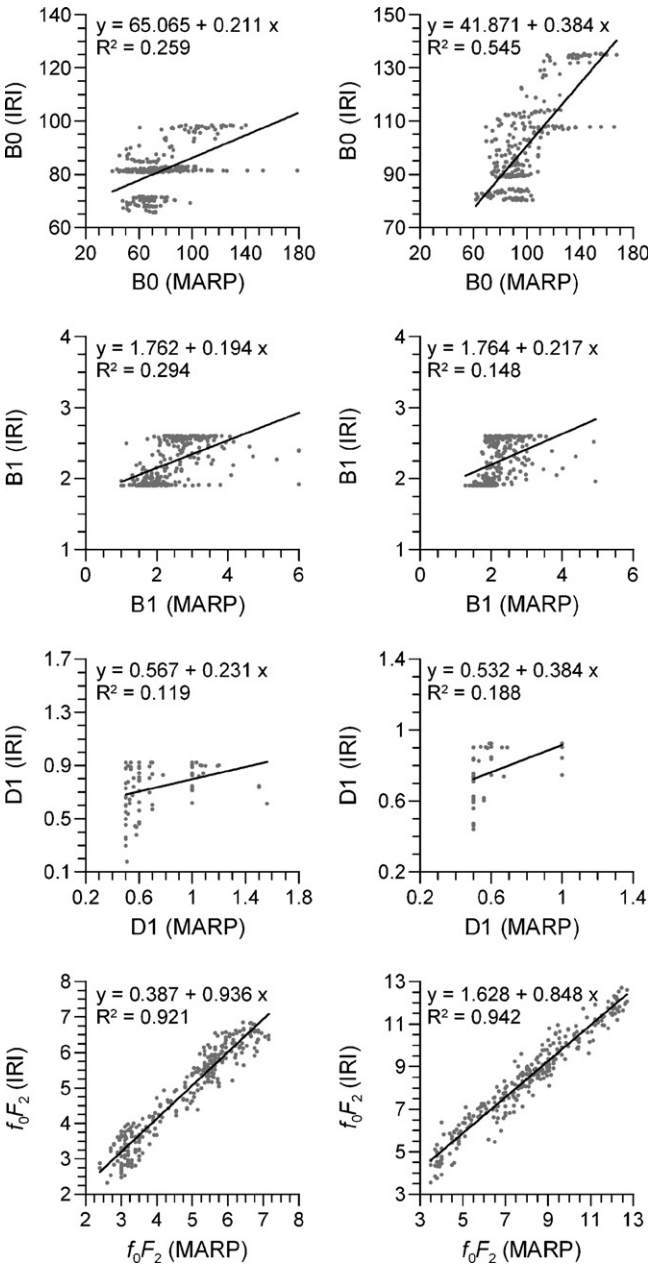

Fig. 2. Scatter plots of indicated *F*-region bottomside parameters and of f_0F_2 obtained by IRI-2001 against the ones obtained from MARP over Ebro station. The plots at the left correspond to year 1995 (low solar activity) and the ones at the right correspond to year 2000 (high solar activity). Solid lines depict the best linear fits of each case, whose equations and coefficients of determination are indicated.

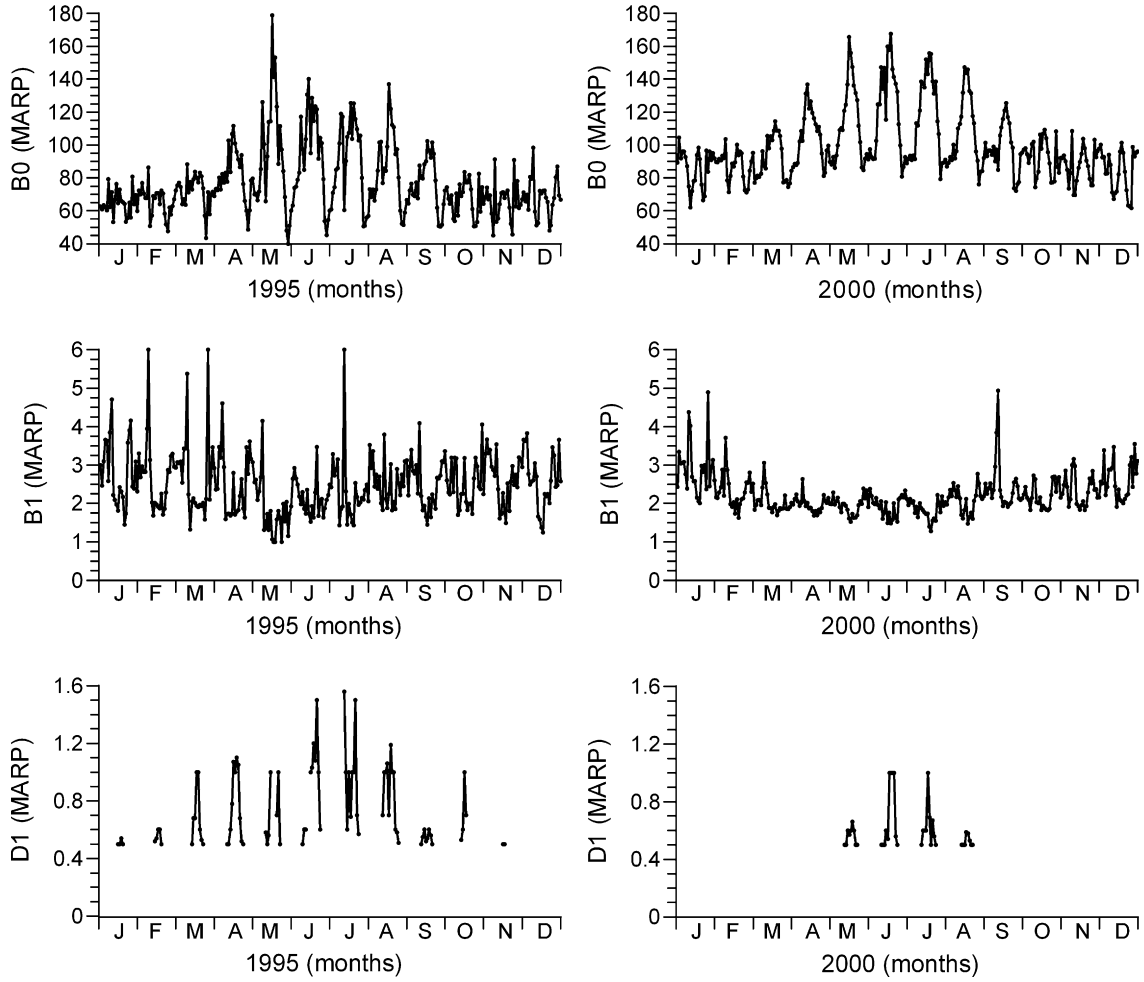

Fig. 3. Daily and annual pattern of the parameters B0, B1 and D1 obtained from MARP over Ebro station for 1995 (left plots) and 2000 (right plots).

files probably linked with disturbed ionospheric conditions. Therefore, for a given month and a given hour we obtain the typical profile expected for quiet ionospheric conditions. Due to the fact that sometimes the B0 and B1 parameters obtained by CARP disagree with those obtained with NHPC for the same ionogram's traces, we recomputed all MARPs by the latest version of NHPC included on SAO-X tool. Fig. 1 depicts an example of the MARP compared with the individual profiles used for its computation. Finally, from the MARP, we extract the parameters B0, B1 and D1 (Huang and Reinisch, 2000; Reinisch and Huang, 2000), to be introduced into the local model.

We use the IRI-2001 model also to obtain IRI B0, B1 and D1 parameters at geographical position corresponding to that of the Ebro Observatory and at coincident times corresponding to that of the MARPs obtained from Ebro data. The IRI modeled parameters are used for comparing with those obtained from MARP and for assessing whether the local model fits better than IRI. Because the MARP represents the typical profile expected for quiet ionospheric conditions, the f_0F_2 storm model was turned off in IRI-2001. The IRI-2001 model has two options for obtaining the B0 and B1 parameters (Bilitza, 1998; Bilitza et al., 2000; Bilitza, 2001): the standard option based on a table of values deduced from ionosonde measurements (Ramakrishnan and Rawer, 1972; Bilitza, 1990), and the Gulyaeva's option based on the half-density height (Gulyaeva, 1987). Comparison of both IRI options against parameters obtained from the MARP have been done, and even thought Gulyaeva's option give more accurate values than standard one for B0 at mid- and low-latitude stations (Bilitza, 1998; Mosert et al., 2004; Zhang et al., 2004), both options revealed large discrepancies with observed data (Sethi and Mahajan, 2002; Lei et al., 2004; Zhang et al., 2004). In present study we used the standard option. The D1 parameter is obtained using $D1 = 2.5C1$ (Reinisch and Huang, 2000), where C1 is given by IRI-2001 software.

3. Modeled parameters and related variations

3.1. Daily and yearly variations

In order to develop our LM and to select the parameters that need better accuracy, we have looked for the IRI-predicted bottomside parameters that show worst agreement comparing with those obtained from MARP. Fig. 2 shows

examples of the comparisons between some parameters obtained by IRI-2001 and MARP. We observe poor agreement for B0, B1 and D1 parameters, all of them having low linear coefficients of determination. The latter confirms the results from Sethi and Mahajan (2002) and Lei et al. (2004). However, there is very good agreement for the f_0F_2. Although not shown here, we did such comparisons for other main ionospheric parameters as h_mF_2, f_0F_1, h_mF_1, f_0E, and h_mE. The preliminary results show that there is reasonable agreement for all of them except h_mE. According to that we focused our efforts to model B0, B1 and D1 parameters at latitudes of the Ebro observatory.

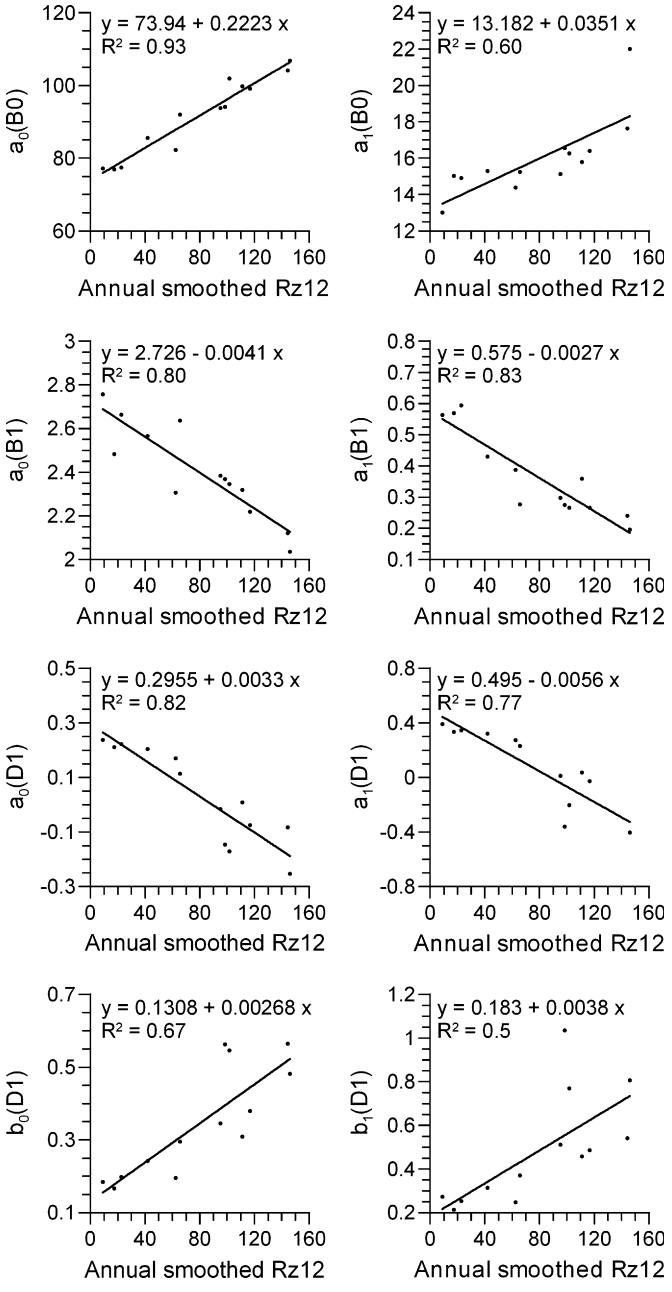

Fig. 4. Solar activity dependence of some of indicated coefficients of Eq. (7). Solid lines depict the best linear fits of each case, whose equations and coefficients of determination are indicated. Note that we consider the yearly average of Rz12 as proxy of the solar activity.

We have obtained the typical time pattern of variation of the above parameters and looked for their systematic variations that could be 'easily' modeled by simple mathematic formulation. We fed LM with the retrospective data from Ebro (1988, 1990, 1991, and from 1995 to 2004) and used the model to predict selected parameters for 2005. The dominant systematic variations have been modeled with harmonic functions obtained by least-square fitting that reconstruct the diurnal, semidiurnal and seasonal variations.

3.1.1. B0 and B1 parameters

B0 is the ionospheric F-region bottomside thickness parameter. According to Bilitza (1998), B0 equals to the difference between the height of the peak of the F_2 layer electron density (h_mF_2) and the height where the electron density equals to 0.24 times of the F_2 layer electron density maximum (N_mF_2). The top plots in the Fig. 3 show a clear diurnal variation of the B0 in summer being noon values generally larger than midnight values (Bilitza et al., 2000; Lei et al., 2004). The latter is even more pronounced for high solar activity. However, semidiurnal variation appears to be dominant in winter. Although not shown here, spectral analysis applied to the time series confirms that periodicities of 24- and 12-h are most prominent. The first step of our LM is to reproduce the above daily variation. For a given month, we obtain the spectral characteristics (amplitude and phase) that fit better the diurnal and semidiurnal variations of the time series:

$$\mathrm{B0} = A + B\cos(\omega_1 t - \psi_1) + C\cos(\omega_2 t - \psi_2), \quad (1)$$

where t means time (0–23 h), $\omega_1 = 2\pi/24$ and $\omega_2 = 2\pi/12$ are the diurnal and semidiurnal angular frequencies, respectively, and ψ_1 and ψ_2 are the diurnal and semidiurnal phases respectively.The coefficients A, B and C mean the daily average of B0, its diurnal and semidiurnal amplitudes, respectively.

B0 also has a clear seasonal trend with minimum values in winter and maximum in summer, and the spring values are usually larger than the fall values (Mosert and Radicella, 1997). It is clear from the top panels of Fig. 3 that for a given year the spectral characteristics display yearly variation, with largest diurnal amplitudes in summer and largest semidiurnal amplitudes in winter. Therefore, we assume that diurnal and semidiurnal amplitudes and background of the B0 parameter are modulated by a seasonal variation. The later is introduced into the second step of our LM by fitting the above coefficients A, B, C, and phases (ψ_1 and ψ_2) to obtain the seasonal variation:

$$A(B)(C) = a + b\cos(\Omega_1 T - \varphi_1) + c\cos(\Omega_2 T - \varphi_2), \quad (2)$$

$$\psi_1(\psi_2) = a' + b'\cos(\Omega_1 T - \varphi_1') + c'\cos(\Omega_2 T - \varphi_2'), \quad (3)$$

where T means time (1–12 month), $\Omega_1 = 2\pi/12$ and $\Omega_2 = 2\pi/6$ are the annual and semi-annual angular frequencies respectively, and φ_1 and φ_2 are the annual and semi-annual phases respectively. The coefficients a, b, and c

Table 1
Coefficients corresponding to the ionospheric *F*-region bottomside parameters B0, B1 and D1, obtained from LM, and threshold values (TH)[a]

	B0	B1	D1	TH
a_0	$73.94 + 0.2223R$	$2.726 - 0.0041R$	$0.2955 - 0.0033R$	–
b_0	14.93	0.2998	$0.1308 + 0.00268R$	–
c_0	6.122	0.1636	–	–
φ_{10}	2.7283	− 0.4587	$2.563 + 0.0031R$	–
φ_{20}	4.8356	0.83	–	–
a_1	$13.182 + 0.0351$R	$0.575 - 0.0027R$	$0.495 - 0.0056R$	$0.353 - 0.0038R + 0.0000242R^2$
b_1	14.645	0.093	$0.183 + 0.0038R$	0.1
c_1	7.382	0.09	–	$0.0373 + 0.0005R$
φ_{11}	2.7627	3.4521	2.875	$2.644 + 0.0036R$
φ_{21}	−1.0599	$2.5099 - 0.0196R$	–	$2.523 - 0.023R$
a_2	6.945	0.297	–	–
b_2	3.014	0.179	–	–
c_2	2.7334	0.1145	–	–
φ_{12}	$3.643 - 0.00338R$	− 0.887	–	–
φ_{22}	1.93	$2.9175 - 0.0149R$	–	–
a'_1	2.252	0.1739	2.986	–
b'_1	1.284	0.398	0.455	–
c'_1	0.681	0.419	–	–
φ'_{11}	2.674	0.605	2.279	–
φ'_{21}	2.4072	1.8488	–	–
a'_2	$0.083 + 0.0033$R	$2.4695 + 0.0067$R	–	–
b'_2	0.568	0.734	–	–
c'_2	0.589	0.645	–	–
φ'_{12}	1.698	− 0.507	–	–
φ'_{22}	0.8494	2.1775	–	–

[a] Note, that R means the annual average of the monthly smoothed sunspot number Rz12.

mean the yearly average of coefficients A, B and C, their annual and semi-annual amplitudes respectively. The coefficients a′, b′ and c′ mean the yearly average of phases (ψ_1 and ψ_2) their annual and semi-annual amplitudes respectively.

The parameter B1 gives the shape of the profile between the two heights from which the B0 is obtained. The larger B1 is the larger densities occur in that region (Bilitza, 1998). The middle panels of the Fig. 3 show that the B1 parameter displays diurnal and semidiurnal variation. The semidiurnal variation is more important in winter and diurnal variation in summer. In this case, noon values are lower than midnight values (Lei et al., 2004), contrary to the daily behavior of the B0. There is also a clear yearly variation of the parameter. The minimum B1 values have been observed during summer and the maximum values have been obtained for winter (Mosert and Radicella, 1997; Lei et al., 2004). As discussed for B0, our local model reproduces the above variations also for the B1 parameter. Eqs. (1)–(3) were applied to obtain similar coefficients to the ones obtained for B0.

3.1.2. D1 parameter

The D1 parameter indicates the presence of the F_1 layer. The diurnal variation of D1 was analyzed by Reinisch and Huang (2000) for several low latitude station-months showing a systematic behavior increasing from zero at sunrise through a maximum at noon and, again, falling down to zero at sunset. In general, at mid-latitudes the F_1 layer is better developed during summer conditions and it is absent during winters of high solar activity. However, F_1 layer use to appear during winters of low solar activity (Buresova et al., 2004). The above behavior is clearly observed from the diurnal/annual course of D1 parameter (bottom panels of Fig. 3), contrary to the diurnal/semidiurnal and annual/semi-annual pattern of the B0 and B1parameters. That is why we avoid semidiurnal and semi-annual variations into our LM for D1 in comparison to the LM obtained for B0 and B1, and Eqs. (4)–(6) are applied to obtain the coefficients that fit better the diurnal and annual variations of the D1 time series:

$$\mathrm{D1} = A + B\cos(\omega_1 t - \psi_1), \tag{4}$$

$$A(B) = a + b\cos(\Omega_1 T - \varphi_1), \tag{5}$$

$$\psi_1 = a' + b'\cos(\Omega_1 T - \varphi'_1). \tag{6}$$

Where t means time (0–23 h), $\omega_1 = 2\pi/24$ is the diurnal angular frequency and ψ_1 is the diurnal phase. The coefficients A and B mean the daily average of D1, and diurnal amplitude, respectively. T means time (1–12 month), $\Omega_1 = 2\pi/12$ is the annual angular frequency and φ_1 is the annual phase. The coefficients a and b mean the yearly average of the coefficients A and B and its annual amplitude, respectively. The coefficients a' and b' mean the yearly average of the phase (ψ_1) and its annual amplitude, respectively.

We have included two boundary conditions into our LM for D1 parameter in order to obtain the D1 coefficients. The magnitude B (Eq. (4)) is forced to be zero for a given month if obtained D1 by MARP is greater that zero for less than four hours only. Magnitude B refers to diurnal amplitude and there is no sense to fit a diurnal

harmonic function to a time series with few data points. Computing D1 daily and yearly variation according to Eqs. (4)–(6) would give D1 different from zero also at nighttime and during winter months at high solar activity. The latter has no sense according to observational facts (bottom panels of Fig. 3). We overcome the above difficulties with D1 modeling by finding a threshold value for the LM of the D1 parameter. This threshold (TH) depends of both, month of year and solar activity level, and for a given month TH is obtained from the fitted D1 values (Eqs. (4)–(6)) at the time t for which MARP D1 differs from zero first time.

3.2. Solar cycle dependence. Local model coefficients

In addition to the daily and yearly patterns mentioned above, the variation of the parameters B0, B1 and D1 depend on solar activity. The latter can be guessed from the Fig. 3. Both, the background and yearly variation that modulate daily variation are different for low and high solar activity. The solar activity dependence is most pronounced in the behavior of D1 parameter and in the behavior of its threshold. Therefore, the solar activity dependence was taken into account in the LM. In order to simplify our LM, we consider the annual average of the monthly mean value of the sunspot number (Rz12) as the solar activity proxy for LM. Hence, the last step of our LM was to search for solar activity dependence of the coefficients described into the Eqs. (1)–(6). The global expansion of these equations can be written as follows for a given parameter P:

$$\begin{aligned} P = {} & a_0 + b_0\cos(\Omega_1 T - \varphi_{10}) + c_0\cos(\Omega_2 T - \varphi_{20}) \\ & + [a_1 + b_1\cos(\Omega_1 T - \varphi_{11}) + c_1\cos(\Omega_2 T - \varphi_{21})] \\ & \times \cos(\omega_1 t - \{a_1' + b_1'\cos(\Omega_1 T - \varphi_{11}') + c_1'\cos(\Omega_2 T - \varphi_{21}')\}) \\ & + [a_2 + b_2\cos(\Omega_1 T - \varphi_{12}) + c_2\cos(\Omega_2 T - \varphi_{22})] \\ & \times \cos(\omega_2 t - \{a_2' + b_2'\cos(\Omega_1 T - \varphi_{12}') + c_2'\cos(\Omega_2 T - \varphi_{22}')\}). \end{aligned} \quad (7)$$

Note that the coefficients c_0, c_1, c_1', a_2, b_2 and c_2, in the LM equals zero for D1. The coefficients, considered to be solar activity dependent are a_0, b_0, c_0, a_1, b_1, c_1, a_2, b_2, c_2, a_1', b_1', c_1', a_2', b_2' and c_2', and the phases φ_{10}, φ_{20}, φ_{11}, φ_{21}, φ_{12}, φ_{22}, φ_{11}', φ_{21}', φ_{12}' and φ_{22}'. The results of solar activity dependence for the above coefficients indicate that a_0(B0), a_0(B1), a_0(D1), b_0(D1), a_1(B0), a_1(B1), a_1(D1), b_1(D1), a_2'(B0), and a_2'(B1), and the phases φ_{10}(D1), φ_{21}(B1), φ_{12}(B0), and φ_{22}(B1), have clear linear trend with the above solar activity proxy. They have significant linear correlation of determination. The other coefficients remain practically constant into our time series and we assume these coefficients to be equal to their respective averages. Fig. 4 shows some results described above. Coefficients of the LM are listed in the Table 1.

Although not shown here, we find that the threshold value (TH) for D1 parameter displays clear seasonal and solar cycle dependence, and it fits to the following empirical law:

$$\mathrm{TH} = a_1 + b_1\cos(\Omega_1 T - \varphi_{11}) + c_1\cos(\Omega_2 T - \varphi_{21}). \quad (8)$$

Where, T means time (1–12 month), $\Omega_1 = 2\pi/12$ and $\Omega_2 = 2\pi/6$ are the annual and semi-annual angular frequencies, respectively, and φ_{11} and φ_{21} are the annual and semi-annual phases, respectively. The coefficients a_1, b_1 and c_1 mean the yearly average of TH, its annual, and semiannual amplitudes, respectively (following the same convention as in Eq. (7)). The result of solar activity dependence analysis for the coefficients from Eq. (8) shows that a_1 follows a power law, c_1, φ_{11} and φ_{21} have a clear linear trend, and b_1 remains practically constant. Table 1 shows also the coefficients of D1 threshold used in our LM.

4. Results

We have calculated the new values of B0, B1 and D1 parameters using the LM explained in the previous section and we compare the original data (MARP) with the results given by IRI-2001 and by LM in order to asses the good-

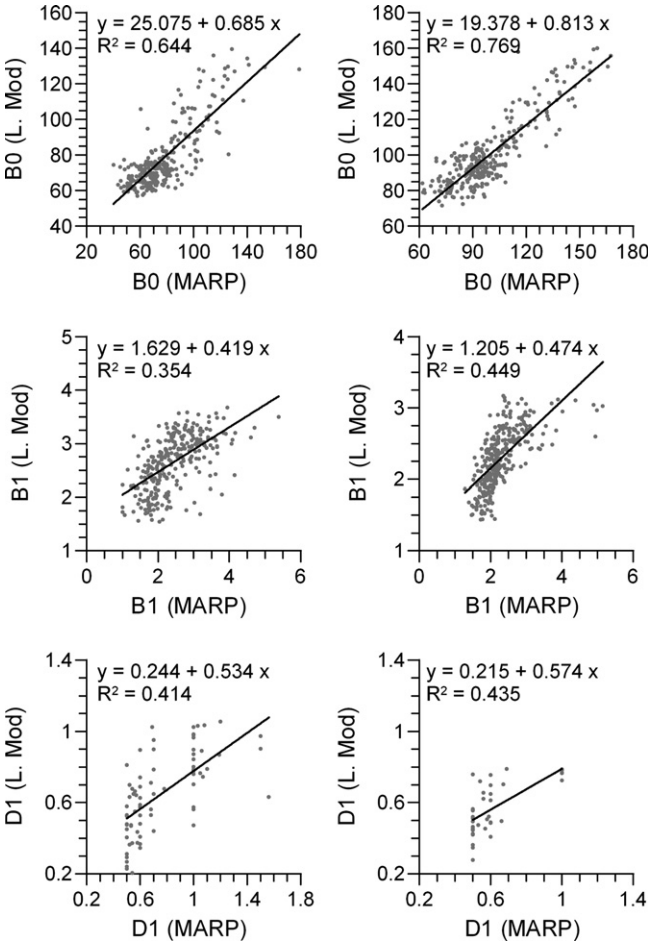

Fig. 5. Scatter plots of indicated F-region bottomside parameters obtained by the Local Model against the ones obtained from MARP over Ebro station. The plots at the left correspond to year 1995 (low solar activity) and the ones at the right correspond to year 2000 (high solar activity). Solid lines depict the best linear fits of each case, whose equations and coefficients of determination are indicated.

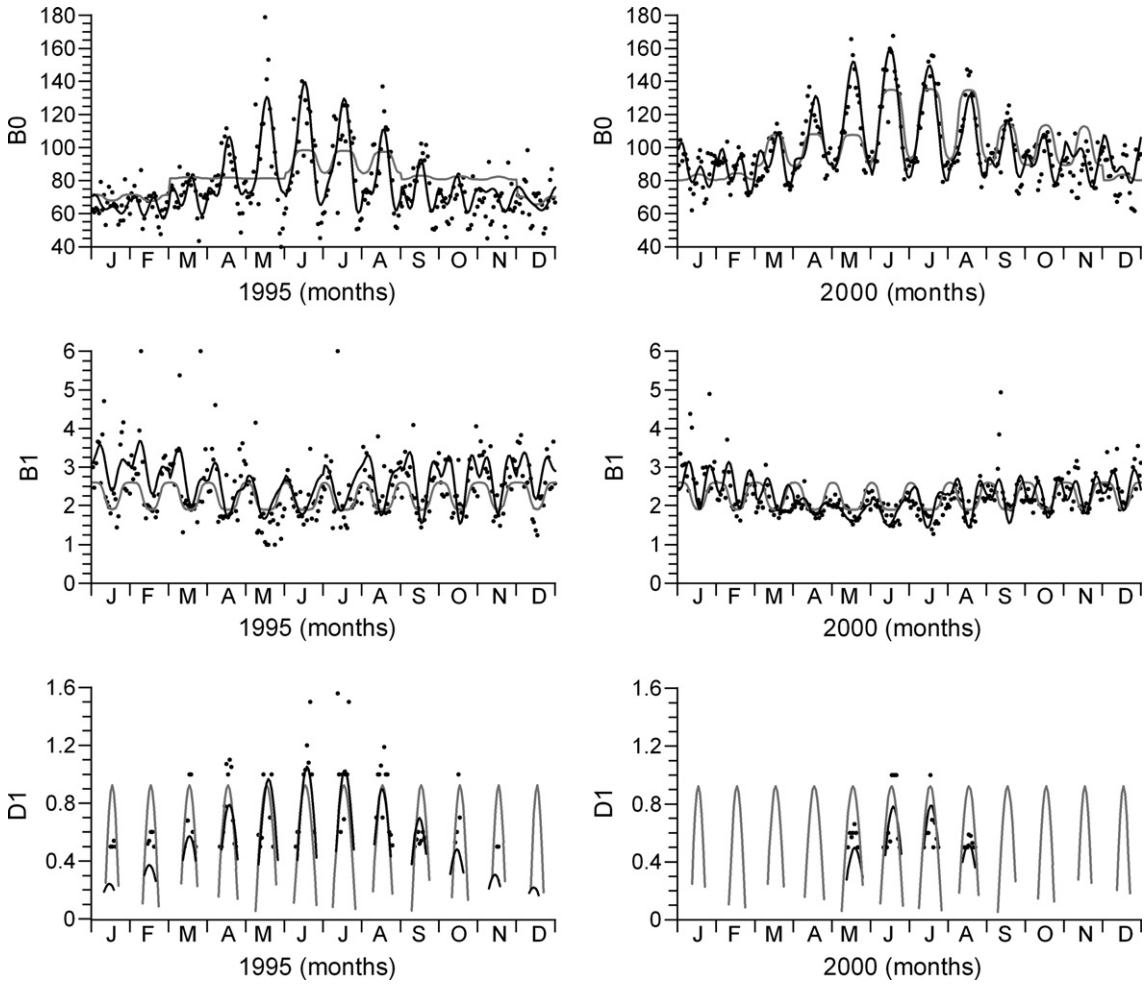

Fig. 6. Comparison daily and yearly course of B0, B1 and D1 parameters obtained from IRI-2001 (grey line), MARP (black dots) and the Local Model (black line) for years of low (left) and high solar activity (right).

ness of LM. The latter is done by feeding the LM with data from June 1988 to December 2004. Fig. 5 shows examples of the comparisons between the parameters obtained by LM and MARP for two levels of sunspot activity. We observe better agreements between LM and MARP (Fig. 5) for all parameters than those reached between IRI-2001 and MARP (Fig. 2). The linear coefficient of determination (R^2) for D1 has been improved by factor 3.6 and 2.6, for B1 the improvement achieved factor 1.3 and 3.0, and the coefficient R^2 for B0 has been improved by factor 2.5 and 1.4 for 1995 and 2000, respectively.

The improvement of LM respect to IRI-2001 is clearly visible from direct comparison between the parameters obtained from both models and MARP (Fig. 6). IRI-2001 gives values for D1 at daytime, reaching the maximum at noon, but with the same diurnal amplitude during the whole year, and it does not follow the annual variation of the diurnal amplitude of D1. It is well known that D1 is better developed during summer (Buresova et al., 2004), and this variation is well represented using LM (Fig. 6 bottom plots). Moreover, D1 has no values during some winter moths, especially at high solar activity. Buresova et al. (2004) stated that in winter months D1 is better developed during low solar activity, and again the latter is reproduced by LM. Fig. 6 shows also that LM follows the diurnal and semidiurnal variation of B1 better than IRI does (middle plots), especially at high solar activity. Moreover, the seasonal variation of diurnal and semidiurnal amplitudes, and background of B1 (Mosert and Radicella, 1997; Lei et al., 2004) is better reproduced by LM than IRI-2001. It is known that B0 is in general larger for high solar activity than for low solar activity (Bilitza et al., 2000). However, the latter is underestimated by IRI-2001 (Fig. 6 top plots). Moreover, IRI-2001 does not follows the semidiurnal variation of B0 and even it underestimates the diurnal variation of B0 during winter and intermediate seasons at low solar activity. The results presented in the top plots of Fig. 6 shows that LM follows the diurnal and semidiurnal variation of B0, and the seasonal variation of diurnal and semidiurnal amplitudes, and background of B0 better than IRI does.

IRI-2001 takes into account the aforementioned sunspot activity dependence. However, it has significant biases for parameters B0 and B1. Sethi and Mahajan (2002) and

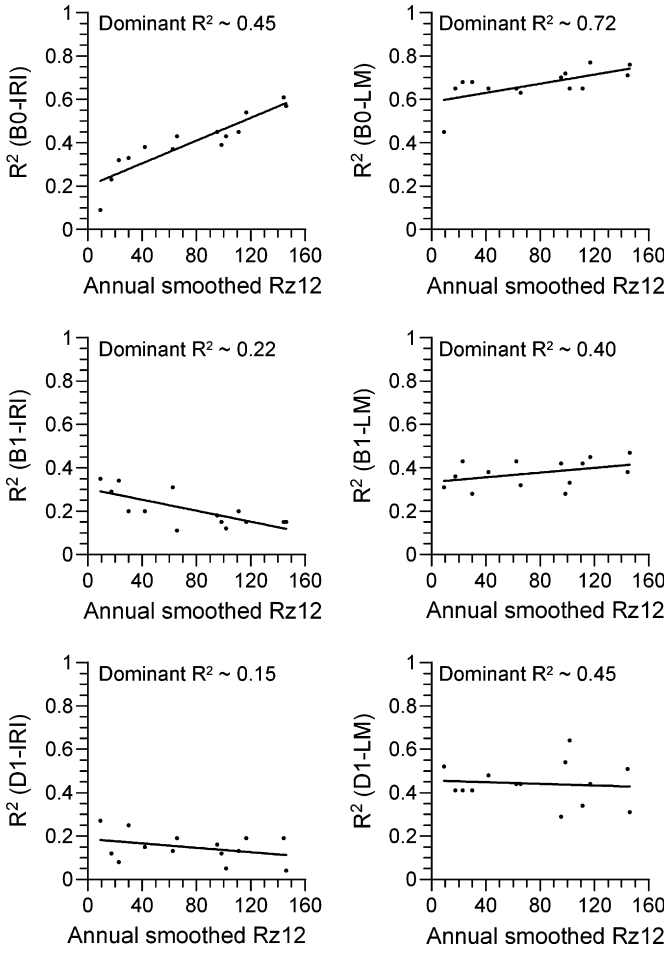

Fig. 7. Solar activity dependence of the linear coefficient of determination (R^2) obtained between IRI-2001 and MARP (left plots), and between LM and MARP (right plots) for B0 (top panels), B1 (middle panels), and D1 (bottom panels). The coefficients R^2 are obtained from best linear fits as indicated in Figs. 2 and 5.

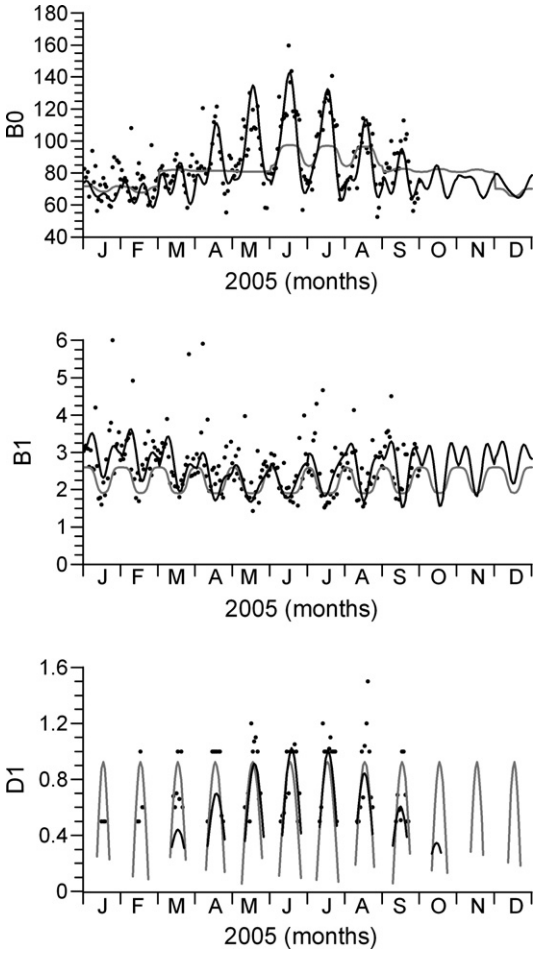

Fig. 8. As Fig. 6, but for year 2005. Note that it has not been used data of 2005 to create LM.

Lei et al. (2004) already noticed a sunspot activity dependence of the linear coefficient of determination between IRI-2001 B0, B1 and D1, and the measured ones. These biases are clearly seen from Fig. 7. We clearly notice from Fig. 7 that the IRI-2001 calculated parameters B0 show better agreement with those, obtained by MARP at high solar activity, while for B1 the agreement is lower. We do not noticed significant dependence of the homogeneity of variances of the IRI and MARP-generated D1 parameters on solar activity. The latter biases are practically overcome with LM, except a small trend of increasing R^2 with sunspot activity for B0 and B1. The latter can be due to the fact that data used to feed LM have more years with high solar activity. However, LM always behaves better than IRI-2001, and the agreement of LM with measured data (MARP) can be improved in average by factor of two for B0 and B1, and by factor of three for D1 compared with IRI-2001.

Up to now we have assessed that LM shows better results than IRI-2001 when compare both models with retrospective data (1988, 1990, 1991, and 1995–2004) that have been used for feeding LM. Now we compare the applicability of the proposed LM for prediction purposes. The model has been tested for January–September, 2005, because for these months we had MARP data. We assumed the annual average of Rz12 to be equal 30. The results of comparison between the parameters obtained by both IRI-2001 and LM models and MARP are depicted in Fig. 8. As discussed above, LM follows the daily and annual course of B0, B1 and D1 better than IRI-2001 does. Although not shown in this paper, we obtained also the linear coefficient of determination (R^2) for the three parameters for all the available data of 2005 in the same way as presented in Figs. 2 and 5. IRI-2001 gives R^2 equal to 0.33, 0.20 and 0.25 for B0, B1 and D1, respectively, whereas LM gives R^2 equal to 0.68, 0.28 and 0.41 for B0, B1 and D1, respectively. Therefore, B0 is improved by factor 2, B1 by factor 1.4, and D1 by factor 1.6 for 2005, respectively.

5. Summary and conclusion

The IRI empirical model is continuously updating to provide better agreement with measured ionospheric data. The latter is done specially during IRI workshops and IRI

Task Force Activities (e.g., Bilitza et al., 2000; Bilitza, 2003; Radicella et al., 1998). Several works show good agreement of IRI model with measured data during quiet period for critical frequencies and heights (e.g., Soicher et al., 1995; Mosert et al., 2004). However; IRI-2001 model has still large discrepancies for ionospheric F region bottomside parameters B0, B1 and D1 (Sethi and Mahajan, 2002; Lei et al., 2004), probably due to the present tabular form of IRI for these parameters. We have developed a Local Model for the above parameters under quiet conditions with a simple mathematical formulation. The LM is based on a least-square fitting to a harmonic function that simulates the diurnal, semidiurnal and seasonal variations according to different levels of solar activity. The LM was created using the retrospective data set of European mid-latitude station Ebro (40.8°N, 0.5°E), which covers more than one solar cycle. The Monthly Averaged Representative Profile (MARP) has been used to obtain the parameters B0, B1 and D1 for quiet ionospheric conditions.

The proposed LM provides more reliable variation of the analyzed bottomside parameters comparing with those IRI-2001-generated. The main advantages of the LM are as follows:

- Better representation of the annual variation of the daily pattern of D1 parameter for all levels of solar activity, excluding an artificial and unreliable occurrence of the F_1 layer during winter time at high solar activity levels, which is found in IRI-2001 model predictions;
- LM takes into account the semidiurnal pattern of B0 and B1 variation during winter time;
- more reliable course of the annual variation of the background levels for both B0 and B1;
- smoothed annual variation of the daily pattern for both B0 and B1, and D1;
- unbiased solar activity dependence of B0 and B1parameters.

In summary, at mid-latitudes and under quiet ionospheric conditions LM allows an improvement of the IRI-2001-predicted coefficients B0 and B1 at an average by factor of two and improvement of the parameter D1predictions by factor of three. To some extent the better behavior of LM compared with IRI was expected because IRI is a global model and LM is a local one valid only for geographical location corresponding to the Ebro Observatory. However, the proposed technique including mathematical formulation could be considered to integrate into further updates of the IRI model. The presented LM has a simple formulation where the coefficients depend on a single parameter, the annual average of Rz12. This makes the model easy to update and to extend to larger geographical region. The latter should be verified by adapting proposed local models for other ionospheric stations located at different longitudes and latitudes, and assessing whether the proposed formulation would improve IRI in a global extent. Therefore, further work is needed for validating the usefulness of such formulation for IRI purposes.

Acknowledgements

The work of D.A. and E.B. is partially supported by Spanish project of MCYT (REN2003-08376-C02-02) and by international cooperation project of CSIC (2004CZ0002). This research was also supported by Grant No1QS300120506 of the Grant Agency of the Academy of Sciences of the Czech Republic.

References

Araujo-Pradere, E.A., Fuller-Rowell, T.J., Codrescu, M.V. Storm: an empirical storm-time ionospheric correction model – 1. Model description. Radio Sci. 37 (3), 1–12, 2002a.

Araujo-Pradere, E.A., Fuller-Rowell, T.J. Storm: an empirical storm-time ionospheric correction model – 2. Validation. Radio Sci. 37 (4), 1–14, 2002b.

Bilitza, D. The International Reference Ionosphere 1990, National Space Science Data Center, NSSDC/WCA-A-R& S Report 90-22, Greenbelt, Maryland, November 1990.

Bilitza, D., Improving the standard IRIB0 model, in: S.M. Radicella (Ed.), Proceedings of the IRI Task Force Activity 1997, pp. 6–14, International Center for Theoretical Physics, Report IC/IR/98/9, Trieste, Italy, 1998.

Bilitza, D., Radicella, S., Reinisch, B., Adeniyi, J., Mosert de Gonzales, M., Zhang, S., Obrou, O. New B0 and B1 models for IRI. Adv. Space Res. 25 (1), 89–96, 2000.

Bilitza, D. International Reference Ionosphere 2000. Radio Sci. 36 (2), 261–275, 2001.

Bilitza, D. International Reference Ionosphere 2000: examples of improvements and new features. Adv. Space Res. 31 (3), 757–767, 2003.

Buresova, D., Altadill, D., Mosert, M., Miró, G. Predicted and measured bottomside F-region electron density and variability of the D1 parameter under quiet and disturbed conditions over Europe. Adv. Space Res. 34, 1973–1981, 2004.

Gulyaeva, T.L. Progress in ionospheric informatics based on electron density profile analysis of ionograms. Adv. Space Res. 10 (6), 39–48, 1987.

Huang, X., Reinisch, B.W. Vertical electron density profiles from the digisonde network. Adv. Space Res. 18 (6), 121–129, 1996a.

Huang, X., Reinisch, B.W. Vertical electron density profiles from digisonde ionograms. The average representative profile. Ann. Geofis. 39 (4), 751–756, 1996b.

Huang, X., Reinisch, B.W. Multiple quasi-parabolic presentation of the IRI profile. Adv. Space Res. 25 (1), 129–132, 2000.

Lei, J., Liu, L., Wan, W., Zhang, S.-R., Holt, J.M. A statistical study of ionospheric profile parameters derived from Millstone Hill incoherent scatter radar measurements. Geophys. Res. Lett. 31, L14804, doi:10.1029/2004GL020578, 2004.

Mosert, M., Radicella, S.M. Seasonal behaviour of B0 and B1, in: Proceedings of the IRI Task Force Activity 1996, pp. 42–49, International Centre for Theoretical Physics, Report IC/IR/97/11, Trieste, Italy, 1997.

Mosert, M., Buresova, D., Ezquer, R., Mansilla, G. Behavior of the bottomside electron density profile over Pruhonice. Adv. Space Res. 34 (9), 1982–1989, 2004.

Press, W.H., Flannery, B.P., Teukolsiy, S.A., Vetterling, W.T. Numerical Recipes: The Art of Scientific Computing. Cambridge University Press, New York, 1986.

Radicella, S.M., Bilitza, D., Reinisch, B.W., Adeniyi, J.O., Mosert Gonzalez, M.E., Zolesi, B., Zhang, M.L., Zhang, S.R. IRI task force

activity at ICTP: Proposed improvements for the IRI region below the peak. Adv. Space Res. 22 (6), 731–739, 1998.

Ramakrishnan, S., Rawer, K. Model electron density profiles obtained by empirical procedures, Space Research XII, pp. 1253–1261, Akademie-Verlag, Berlin, 1972.

Reinisch, B.W., Huang, X. Redefining the IRI F1 layer profile. Adv. Space Res. 25 (1), 81–88, 2000.

Reinisch, B.W., Huang, X., Galkin, I.A., Paznukhov, V., Kozlov, A. Recent advances in real-time analysis of ionograms and ionospheric drift measurements with digisondes. J. Atmos. Sol. Terr. Phys. 67, 1054–1062, doi:10.1016/j.jastp.2005.01.009, 2005.

Sethi, N.K., Mahajan, K.K. The bottomside parameters B0, B1 obtained from incoherent scatter measurements during a solar maximum and their comparisons with the IRI-2001 model. Ann. Geophys. 20 (6), 817–822, 2002.

Soicher, H., Gorman, F., Tsedilina, E.E., Weitsman, O.V. Comparison of the IRI-90 with measured ionospheric parameters at midlatitudes. Adv. Space Res. 16 (1), 129–132, 1995.

Zhang, M.L., Shi, J.K., Wang, X., Wu, S.Z., Zhang, S.R. Comparative study of ionospheric characteristic parameters obtained by DPS-4 digisonde with IRI2000 for low latitude station in China. Adv. Space Res. 33, 869–873, 2004.